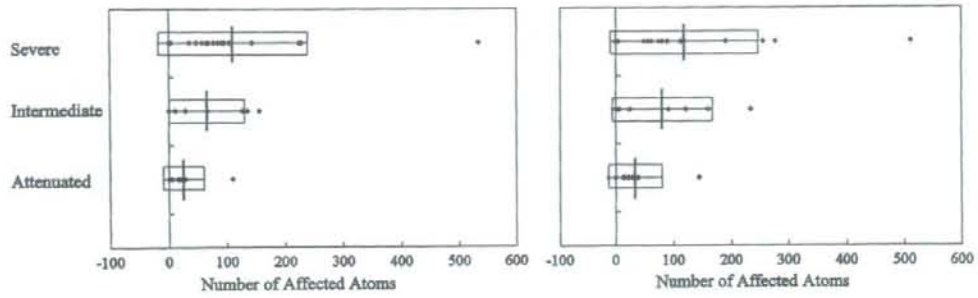

Fig. 2 Numbers of atoms influenced by amino acid substitutions found in severe, intermediate, and attenuated mucopolysaccharidosis type I (MPS I) cases. Main chain (*left*) and side chain (*right*). *Boxes* indicate mean ± standard deviation

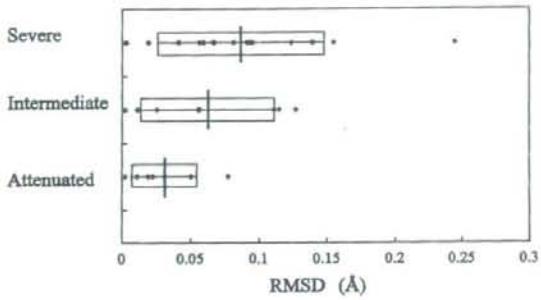

Fig. 3 Root-mean-square distance (RMSD) for severe, intermediate, and attenuated mucopolysaccharidosis type I (MPS I) mutations (Å). *Boxes* indicate mean ± standard deviation

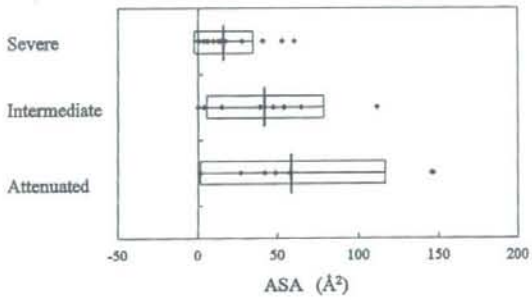

Fig. 4 Solvent-accessible surface area (ASA) of amino acid residues associated with severe, intermediate, and attenuated mucopolysaccharidosis type I (MPS I) (Å^2). *Boxes* indicate mean ± standard deviation

influences. The results are shown in Fig. 3. Those for the severe, intermediate, and attenuated groups were 0.087, 0.063, and 0.030 Å, respectively. Results of the F test and Welch's t test showed that there was a significant difference in RMSD between the severe MPS I and attenuated groups ($P < 0.05$) and between the severe and milder ones (the intermediate and attenuated groups) ($P < 0.05$). No significant difference in the average RMSD between the severe and intermediate groups or between the intermediate and attenuated ones could be found.

ASA of amino acid residues associated with MPS I mutations

To determine locations of the residues associated with MPS I mutations in the structure of IDUA, ASA values of the residues in the wild-type structure were calculated, the results being summarized in Fig. 4 (The result for each residue is shown in the "Supplementary" data). In the severe MPS I group, the ASA range extended to 0.0–60.1 Å^2, the average being 16.0 Å^2. In the attenuated group, the ASA range extended to 0.8–146.6 Å^2, the average being 58.6 Å^2. The results of the F test ($P < 0.05$) and Welch's t test ($P < 0.05$) showed that there was a significant difference between the two groups. The average ASA in the intermediate group was 41.8 Å^2, indicating that it had an intermediate value between those in the severe and attenuated groups. The F test and Welch's t test revealed that there was a significant difference between severe MPS I and milder ones (intermediate and attenuated) ($P < 0.05$). There was also a significant difference in the average ASA between the severe and intermediate ones although not between the intermediate group and the attenuated one. These results indicate that the residues associated with severe MPS I mutations tend to be less solvent-accessible than those associated with the milder MPS I mutations.

Color imaging of structural changes for representative amino acid substitutions causing MPS I

Regarding MPS I mutations, we paid attention to P496R, H240R, and E182K and examined structural changes by means of color imaging. The results are shown in Fig. 5. As shown in Fig. 5a, P496 is buried, and the atoms influenced by P496R are located throughout the whole enzyme. On the other hand, H240 is located on the surface of the

enzyme protein, and the number of atoms influenced by H240R is limited, as shown in Fig. 5b. Furthermore, color imaging clearly revealed that the active site pocket was severely affected by E182K, as shown in Fig. 5c.

Discussion

Although a large number of gene mutations causing MPS I have been reported, structural information on a defective IDUA protein is sparse. To elucidate the basis of MPS I, it is very important to examine the structural changes in the enzyme protein responsible for the different phenotypes.

We constructed structural models of MPS I mutant enzyme proteins and examined the correlation between the structural changes and the phenotypes by means of calculation of the numbers of atoms influenced by amino acid substitutions and determination of the RMSD and ASA. Considering the results, the residues associated with severe MPS I mutations tend to be located in the core region of the enzyme protein, and the structural changes are large, which would seriously affect protein folding and/or intracellular transport, which would lead to degradation of the enzyme protein by the endoplasmic reticulum's quality control (ERQC) system before it is transported to the lysosome, as indicated in other lysosomal diseases, including Tay-Sachs disease (Mahuran 1999). Among the mutations responsible for the severe phenotype, the numbers of atoms influenced by A75T, L218P, I270S, and A327P are exceptionally small. However, for L218P and A327P, the ASA values are small, indicating that the substituted residues are buried. The buried residues affected are predicted to cause serious conformation changes, which would affect the stability of the enzyme and result in the severe phenotype.

On the other hand, small structural changes on the surface of the enzyme protein were generally found in the attenuated form. This suggests that at least a small amount of the mutant enzyme can be protected from the ERQC system and transported to the lysosome without losing its activity, and this must lead to residual IDUA activity and thus the late-onset attenuated phenotype. An exceptional case to this "rule" is R89Q. This mutation has been identified in nine of 38 Japanese MPS I alleles (Yamagishi et al. 1996) and also observed in Caucasian Scheie alleles (Scott et al. 1992). The expression study revealed that R89Q was a destabilizing amino acid substitution producing an IDUA protein that had a reduced ability to bind and/or to turn over a substrate (Scott et al. 1992). However, it remains unclear why the predicted structural change results in residual enzyme activity.

From the results of examination of the intermediate form combined with those for the severe and attenuated groups, the structural changes in the enzyme protein are thought to be correlated with the severity of the phenotype in MPS I.

Color imaging clearly showed the characteristic structural changes caused by the representative amino acid substitutions. P496R causes a large structural change in the core region of the enzyme, which must lead to destabilization and degradation of the expressed protein, resulting in the severe phenotype. H240R is predicted to cause a small structural change on the molecular surface of the protein and thus not to affect the active site. This suggests that at least a small amount of mutant protein having enzyme activity can be protected from the ERQC system and transported to the lysosome, leading to the attenuated phenotype. Color imaging of the atoms in the mutant IDUR with E182K clearly showed a structural change in the active site pocket. Brooks et al. expressed the E182K mutant protein in CHO-K1 cells and found that the expressed protein was enzymatically inactive (Brooks et al. 2001), suggesting that E182K leads to the severe phenotype.

In conclusion, we examined the structural changes in IDUA caused by MPS I mutations. The results show the correlation between the structural changes and clinical phenotypes. Structural investigation is useful for elucidating the basis of MPS I and for increasing our ability to predict the clinical outcome of the disease.

Fig. 5 Color imaging of the atoms in the three-dimensional structure influenced by representative amino acid substitutions causing mucopolysaccharidosis type I (MPS I). The degrees and distributions for P496R (**a**), H240R (**b**), and E182K (**c**) are shown. Each atom is colored according to the distance between the atom in the mutant and the corresponding atom in the wild-type structure. The colors of the atoms show the distances, as follows: *blue* < 0.15 Å, 0.15 Å $\leq$ *cyan* < 0.30 Å, 0.30 Å $\leq$ *green* < 0.45 Å, 0.45 Å $\leq$ *yellow* < 0.60 Å, 0.60 Å $\leq$ *orange* < 0.75 Å, and *red* ≥ 0.75 Å

Acknowledgments We thank Dr. J. Ponder (Department of Biochemistry and Molecular Biophysics, Washington University) for providing us with the TINKER software. We also thank I.K. McDonald, D. Naylor, D. Jones, J.M. Thornton, S. Hubbard, D.K. Smith, R. Laskowski, and G. Hutchinson for providing us with the HBPLUS. This work was partly supported by grants from the Japan Society for the Promotion of Science, the Ministry of Education, Science, Sports and Culture of Japan, the Ministry of Health and Welfare of Japan, the Japan Science and Technology Agency, and CREST.

References

Beesley CE, Meaney CA, Greenland G, Adams V, Vellodi A, Young EP, Winchester BG (2001) Mutational analysis of 85 mucopolysaccharidosis type I families: frequency of known mutations, identification of 17 novel mutations and in vitro expression of missense mutations. Hum Genet 109:503–511

Brooks DA (1993) Review: the immunochemical analysis of enzyme from mucopolysaccharidoses patients. J Inher Metab Dis 16:3–15

Brooks DA, Fabrega S, Hein LK, Parkinson EJ, Durand P, Yogalingam G, Matte U, Giugliani R, Dasvarma A, Eslahpazire J, Henrissat B, Mornon JP, Hopwood JJ, Lehn P (2001) Glycosidase active site mutations in human α-L-iduronidase. Glycobiology 11:741–750

Brooks DA (2002) α-L-Iduronidase and enzyme replacement therapy for mucopolysaccharidosis I. Expert Opin Biol Ther 2:967–976

Bunge S, Kleijer WJ, Steglich C, Beck M, Zuther C, Morris CP, Schwinger E, Hopwood JJ, Scott HS, Gal A (1994a) Mucopolysaccharidosis type I: identification of 8 novel mutations and determination of the frequency of the two common alpha-L-iduronidase mutations (W402X and Q70X) among European patients. Hum Mol Genet 3:861–866

Bunge S, Steglich C, Kleijer WJ (1994b) Mucopolysaccharidosis type I. Identification of 93% of mutant alleles in a group of 70 patients. Am J Hum Genet 55:44

Clarke LA, Nelson PV, Warrington CL, Morris CP, Hopwood JJ, Scott HS (1994) Mutation analysis of 19 North American mucopolysaccharidosis type I patients: identification of two additional frequent mutations. Hum Mutat 3:275–282

Dudek MJ, Ponder JW (1995) Accurate modeling of the intramolecular electrostatic energy of proteins. J Comput Chem 16:791–816

Kabsch W (1976) A solution for the best rotation to relate two sets of vectors. Acta Crystallogr A32:827

Kabsch W (1978) A discussion of the solution for the best rotation to relate two sets of vectors. Acta Crystallogr A34:922–923

Kong MJ, Ponder JW (1997) Reaction field methods for off-center multipoles. J Chem Phys 107:481–492

Kundrot CE, Ponder JW, Richards FM (1991) Algorithms for calculating excluded volume and its derivative as a function of molecular conformation and their use in energy minimization. J Comput Chem 12:402–409

Laradi S, Tukel T, Erazo M, Shabbeer J, Chkioua L, Khedhiri S, Ferchichi S, Chaabouni M, Miled A, Desnick RJ (2005) Mucopolysaccharidosis I: alpha-L-iduronidase mutations in three Tunisian families. J Inherit Metab Dis 28:1019–1026

Lee-Chen GJ, Wang TR (1997) Mucopolysaccharidosis type I: identification of novel mutations that cause Hurler/Scheie syndrome in Chinese families. J Med Genet 34:939–941

Li P, Wood T, Thompson JN (2002) Diversity of mutations and distribution of single nucleotide polymorphic alleles in the human alpha-L-iduronidase (IDUA) gene. Genet Med 4:420–426

Mahuran DJ (1999) Biochemical consequences of mutations causing the GM2 gangliosidosis. Biochem Biophys Acta 1455:105–108

Matsuzawa F, Aikawa S, Sakuraba H, Lan HT, Tanaka A, Ohono K, Sugimoto Y, Ninomiya H, Doi H (2003) Structural basis of the GM2 gangliosidosis B variant. J Hum Genet 48:582–589

Matsuzawa F, Aikawa S, Doi H, Okumiya T, Sakuraba H (2005) Fabry disease: correlation between structural changes in α-galactosidase, and clinical and biochemical phenotype. Hum Genet 117:317–328

Matte U, Yogalingam G, Brooks D, Leistner S, Schwartz I, Lima L, Norato DY, Brum JM, Beesley C, Winchester B, Giugliani R, Hopwood JJ (2003) Identification and characterization of 13 new mutations in mucopolysaccharidosis type I patients. Mol Genet Metab 78:37–43

McDonald IK, Thornton JM (1994) Satisfying hydrogen bonding potential in proteins. J Mol Biol 238:777–793

Neufeld EF, Muenzer J (2001) The mucopolysaccharidoses. In: Scriver CR, Beaudet AL, Sly WS, Valle D (eds) The metabolic and molecular bases of inherited disease, 8th edn. McGraw-Hill, New York, pp 3421–3452

Pappu RV, Hart RW, Ponder JW (1998) Analysis and application of potential energy smoothing for global optimization. J Phys Chem B102:9725–9742

Rempel BP, Clarke LA, Withers SG (2005) A homology model for human α-L-iduronidase: insights into human disease. Mol Genet Metab 85:28–37

Ren P, Ponder JW (2003) Polarizable atomic multipole water model for molecular mechanics simulation. J Phy Chem B107:5933–5947

Sakuraba H, Matsuzawa F, Aikawa S, Doi H, Kotani M, Lin H, Ohno K, Tanaka A, Yamada H, Uyama E (2000) Molecular and structural studies of the GM2 gangliosidosis O variant. J Hum Genet 47:176–183

Sakuraba H, Matsuzawa F, Aikawa S, Doi H, Kotani M, Nakada H, Fukushige T, Kanzaki T (2004) Structural and immunocytochemical studies on α-*N*-acetylgalactosaminidase deficiency (Schindler/Kanzaki disease). J Hum Genet 49:1–8

Scott HS, Ashton LJ, Eyre HJ, Backer E, Brooks DA, Callen DF, Sutherland GR, Morris CO, Hopwood JJ (1990) Chromosomal localization of the human α-L-iduronidase (IDUA) to 4p16.3. Am J Hum Genet 47:802–807

Scott HS, Guo X-H, Hopwood JJ, Morris CP (1992) Structure and sequence of the α-L-iduronidase gene. Genomics 13:1311–1313

Scott HS, Litjens T, Nelson PV, Thompson PR, Brooks DA, Hopwood JJ, Morris CP (1993) Identification of mutations in the alpha-L-iduronidase gene (IDUA) that cause Hurler and Scheie syndromes. Am J Hum Genet 53:973–986

Scott HS, Bunge S, Gal A, Clarke LA, Morris CP, Hopwood JJ (1995) Molecular genetics of mucopolysaccharidosis type I: diagnostic, clinical, and biological implications. Hum Mutat 6:288–302

Teng YN, Wang TR, Hwu WL, Lin SP, Lee-Chen GJ (2000) Identification and characterization of -3c-g acceptor splice site mutation in human alpha-L-iduronidase associated with mucopolysaccharidosis type IH/S. Clin Genet 57:131–136

Tieu PT, Bach G, Matynia A, Hwang M, Neufeld EF (1995) Four novel mutations underlying mild or intermediate forms of alpha-L-iduronidase deficiency (MPS IS and MPS IH/S). Hum Mutat 6:55–59

Tylor JA, Gibson GJ, Brooks DA, Hopwood JJ (1991) α-L-iduronidase in normal and mucopolysaccharidosis type I human skin fibroblasts. Biochem J 274:263–268

Venturi N, Rovelli A, Parini R, Menni F, Brambillasca F, Bertagnolio F, Uziel G, Gatti R, Filocamo M, Donati MA, Biondi A, Goldwurm S (2002) Molecular analysis of 30 mucopolysaccharidosis type I patients: evaluation of the mutational spectrum in Italian population and identification of 13 novel mutations. Hum Mutat 20:231

Weiner SJ, Kallman PA, Case DA, Singh UC, Ghio C, Alagona G, Profeta S, Weiner P (1984) A new force field for molecular mechanical simulation of nucleic acids and proteins. J Am Chem Soc 106:765–784

Yamagishi A, Tomatsu S, Fukuda S, Uchiyama A, Shimozawa N, Suzuki Y, Kondo N, Sukegawa K, Orii T (1996) Mucopolysaccharidosis type I: identification of common mutations that cause Hurler and Scheie syndrome in Japanese populations. Hum Mut 7:23–29

Yogalingam G, Guo XH, Muller VJ, Brooks DA, Clements PR, Kakkis ED, Hopwood JJ (2004) Identification and molecular characterization of alpha-L-iduronidase mutations present in mucopolysaccharidosis type I patients undergoing enzyme replacement therapy. Hum Mutat 24:199–207

European Journal of Haematology ISSN 0902-4441

ORIGINAL ARTICLE

Possible application of flow cytometry for evaluation of the structure and functional status of WASP in peripheral blood mononuclear cells

Masaru Nakajima[1,3], Masafumi Yamada[2], Koji Yamaguchi[3], Yukio Sakiyama[3], Atsushi Oda[4], David L. Nelson[5], Yasutaka Yawaka[1], Tadashi Ariga[2]

[1]Division of Oral Functional Science, Department of Dentistry for Children and Disabled Person, Hokkaido University Graduate School of Dental Medicine, Sapporo, Japan; [2]Department of Pediatrics, Hokkaido University Graduate School of Medicine, Sapporo, Japan; [3]Research Group of Human Gene Therapy, Hokkaido University, Graduate School of Medicine, Sapporo, Japan; [4]Department of Preventive Medicine, Hokkaido University School of Medicine, Sapporo, Japan; [5]National Institutes of Health, National Cancer Institute, Metabolism Branch, Bethesda, MD, USA

Abstract

The Wiskott-Aldrich syndrome protein (WASP), which is defective in Wiskott-Aldrich syndrome (WAS) patients, is an intracellular protein expressed in non-erythroid hematopoietic cells. Previously, we have established methods to detect intracellular WASP expression in peripheral blood mononuclear cells (PBMNCs) using flow cytometric analysis (FCM-WASP) and have revealed that WAS patients showed absent or very low level intracellular WASP expression in lymphocytes and monocytes, while a significant amount of WASP was detected in those of normal individuals. We applied these methods for diagnostic screening of WAS patients and WAS carriers, as well as to the evaluation of mixed chimera in WAS patients who had previously undergone hematopoietic stem cell transplantation. During these procedures, we have noticed that lymphocytes from normal control individuals showed dual positive peaks, while their monocytes invariably showed a single sharp WASP-positive peak. To investigate the basis of the dual positive peaks ($WASP^{low\text{-}bright}$ and $WASP^{high\text{-}bright}$), we characterized the constituent linage lymphocytes of these two WASP-positive populations. As a result, we found each $WASP^{low/high}$ population comprised different linage PBMNCs. Furthermore, we propose that the difference between the two WASP-positive peaks did not result from any difference in WASP expression in the cells, but rather from a difference in the structural and functional status of the WASP protein in the cells. It has been shown that WASP may exist in two forms; an activated or inactivated form. Thus, the structural and functional WASP status or configuration could be evaluated by flow cytometric analysis.

Key words Wiskott-Aldrich syndrome protein; flow cytometry; Wiskott-Aldrich syndrome; peripheral blood mononuclear cells

Correspondence Tadashi Ariga, Department of Pediatrics, Hokkaido University Graduate School of Medicine, Japan. Tel: +81-11-706-7153; Fax: +81-11-706-7898; e-mail: tada-ari@med.hokudai.ac.jp

Accepted for publication 19 October 2008

doi:10.1111/j.1600-0609.2008.01180.x

The Wiskott-Aldrich syndrome protein (WASP) is the causative molecule underlying WAS (1). WASP comprises 502 amino acid residues, and is encoded by the *WASP gene*, which is organized into 12 exons encompassing 9 kb gDNA, and is located on the X-chromosome at Xp11.23-p11.22 (2). WASP belongs to the growing family of WASP/Scar/WAVE cytoplasmic scaffolding proteins, which are involved in cytoskeleton remodeling and actin nucleation/polymerization in response to activation stimuli (3, 4). Recent studies have revealed that WASP interacts with a number of intracellular molecules and plays key roles in signal transduction and the regulation of actin-polymerization (5–9). Furthermore, on the basis of crystal structure studies of the WASP molecule, it has been shown that WASP is involved in an auto-inhibition and activation mechanism via intra-molecular conformation changes (10).

Loss of function mutations in the *WASP* genes causes WAS, and X-linked thrombocytopenia (XLT) (11, 12), while gain of function mutations in the WASP gene have shown to cause X-linked neutropenia (XLN) (13). However, the full extent of the varied clinical symptoms observed in these patients (14–20) has not been fully elucidated in relation to WASP abnormalities.

Previously, we have established methods to detect intracellular WASP expression in peripheral blood mononuclear cells (PBMNCs) by flow cytometric analysis (FCM-WASP) (21). We have applied the methods to the screening of WAS patients, for the identification of carrier (22–24), or for the evaluation of WAS patients after receiving hematopoietic stem cell transplantation (25) and finally to detection of spontaneous reversion of WAS cases (26). During these pervious FCM-WASP experiments, we have identified normal control individual lymphocytes that showed dual positive peaks (WASP$^{low\text{-}bright}$ and WASP$^{high\text{-}bright}$). In this study, we tried to characterize the constituent cell lineage members of these two distinct populations of normal lymphocytes as detected by FCM-WASP, and investigate the mechanism underlying the two populations. Here we demonstrate that the two WASP populations consist of different lineage lymphocytes, and the difference between the two WASP$^{low/high}$ lymphocyte populations seems to result from differences in the functional status of the WASP molecule in the cell.

Materials and methods

Anti-WASP antibodies

Two different anti-WASP antibodies were used in this study. One is 3F3A5 (1.2 mg/mL), unconjugated mouse-IgG1 monoclonal anti-WASP antibody (11), which was raised against recombinant WASP corresponding to amino acids 202–302. We used 3F3A5 for FCM-WASP with fluorescein isothiocyanate (FITC)-conjugated goat anti-mouse IgG1 antibody (Southern Biotechnology Associates, Birmingham, AL, USA, 1.0 mg/mL). The second antibody was B-9 (Santa Cruz Biotechnology, Inc, 200 μg/mL), a phycoerythrin (PE)-conjugated mouse monoclonal IgG2a antibody, which was raised against recombinant WASP corresponding to amino acids 1–250.

FCM-WASP

FCM-WASP was performed as previously described (21). In brief, PBMNCs were purified using Ficoll-Hypaque, and both the cell surface and cytoplasm were stained. For staining cytoplasmic WASP, cells were treated with Cytofix/Cytoperm solution from the CytoStain kit (Pharmingen, San Diego, CA, USA) at 4°C for 20 min. After two washes with Perm/Wash solution (Pharmingen), they were incubated with 200× diluted mouse anti-WASP antibody (3F3A5) or 5× diluted mouse IgG1 antibody (BectonDickinson, San Jose, CA, USA) at 4°C for 30 min. After washing in phosphate-buffer saline (PBS)-2% fetal bovine serum (P-2), they were incubated with 100× diluted goat anti-mouse IgG1-FITC antibody (Southern Biotechnology Associates) as the secondary antibody again at 4°C for 30 min. In some experiments, a second, 10× diluted different anti-WASP antibody (B-9) was used. We used 10× diluted PE-conjugated mouse IgG2 as an isotypic control antibody. For surface/intracellular dual staining using the 3F3A5 antibody, we first stained the cell surface, followed by washing twice before performing intracellular staining. Antibodies used for surface staining were as follows; 5 μL of PE-conjugated anti-CD4, 10 μL of anti-CD8, and 10 μL of anti-CD56 (Southern Biotechnology Associates); PE-conjugated 10 μL of anti-CD20 (Beckman Coulter, Fullerton, CA, USA); and 10 μL of PE-Cy5-conjugated anti-CD45RA and 10 μL of anti-CD45RO (eBioscience, San Diego, CA, USA). The antibodies or the cell surface staining were mouse IgG2 to avoid cross reactivity with the 100× diluted goat anti-mouse IgG1-FITC antibody. We washed it with P-2 twice and stained intracellular WASP as described above. Stained PBMNCs were analyzed by FACSCalibur (BD, San Jose, CA, USA), using CellQuest software (Becton Dickinson).

Simultaneous staining with the two anti-WASP antibodies

After fixation and permeabilization procedure, normal control individual lymphocytes were simultaneously stained with 3F3A5 and B-9 at 4°C for 30 min, followed by staining with goat anti-mouse IgG1-FITC, and then, FCM-WASP was performed. The two WASP antibodies were used at the same protein concentration.

CD3+/CD45RA+ and CD3+/CD45RO+ purification

The two populations of CD3+/CD45RA+ and CD3+/CD45RO+ were purified as follows. Twenty microliters of CD3, CD45RA or CD45RO MicroBeads (Miltenyi Biotec, Bergisch Gladbach, Germany) diluted with 80 μL of magnetic cell sorting (MACS) buffer (pH 7.2, PBS 0.5% BSA, 2 mM EDTA) were incubated with each batch of 10^7 lymphocytes at 4°C for 15 min, and then, these cells were washed in MACS buffer. Afterwards, the two populations prepared as above were separated with Vario MACS (Miltenyi Biotec) and an MS

column (Miltenyi Biotec). Each cell population was checked for purity by flow cytometry.

Western blot analysis

The CD3+CD45RA+ ($WASP^{low\text{-}bright}$) lineages and CD3+CD45RO+ ($WASP^{high\text{-}bright}$) cells were respectively dissolved in RIPA buffer (Sigma, St Louis, MO, USA) containing protease inhibitors at 4°C for 20 min and were centrifuged at 14 500 *g* at 4°C for 20 min. We completely dissolved the cells in SD sample buffer (Sigma) and after boiling the samples, the cell extract of comprising 5×10^6 equivalency was electrophoresed with 10% polyacrylamide gel and blotted on a Hybond-PPVDF membrane (Amersham, Buckinghamshire, UK). We then stained the membrane with 1000× diluted 3F3A5 and 250× diluted anti-WIP antibody (kindly provided by Dr Ramesh N, Children's Hospital, Harvard University, MA, USA) as a loading control, followed by 1000× diluted peroxidase-conjugated goat anti-mouse IgG and 1000× diluted peroxidase-conjugated goat anti-rabbit IgG, and then used the ECL detection system (Amersham, Aylesbury, UK) for the detection of bands.

RT-PCR analysis

Total RNA from CD3+CD45RA+cells or CD3+CD45RO+ cells was extracted using an RNA isolation solvent (RNA zolTM Cinna/Biotecx, Houston, TX, USA). Two micrograms each of total RNA was used for cDNA synthesis with the first-strand cDNA synthesis kit (Pharmacia LKB Biotechnology, Uppsala, Sweden) and then, the same volume of each part of cDNA product was PCR-amplified with a set of primers (forward: GAAGACAAGGGCAGAAAGCA, reverse: GGGTTATCCTTCACGAAGCA). We performed electrophoresis of the PCR products and photographed the bands stained with ethidium bromide in the gel under ultraviolet light.

FCM-WASP for CD8+ lymphocytes after *in vitro* short-term activation

The change of WASP-positive pattern in CD8+ lymphocytes was studied after *in vitro* short-term activation. CD8+ cells were purified in the following way. PBMNCs from normal individuals were incubated at 4°C with each 20 μL of CD4, CD56 and CD20 MicroBeads (Miltenyi Biotec) for 15 min, and cells were obtained after performing Vario MACS using an LD column and their purity was checked and used for the experiment. After *in vitro* short-term activation with ionomycin (25 ng/mL) and PMA (1 μg/mL) at 37°C for 4 h, CD8+ lymphocytes were performed FCM-WASP and analyzed by CellQuest software (Franklin Lakes, NJ, USA).

Results

Normal peripheral blood mononuclear cells showed two WASP-positive populations by FCM-WASP

We have detected two WASP-positive populations; $WASP^{low\text{-}bright}$ and $WASP^{high\text{-}bright}$, in normal PBMNCs using 3F3A5. In monocytes, these two distinct populations have never been detected, but only low-bright positive have been previously described. The pattern of these dual positive peaks showed some variation among individuals (Fig. 1). We first studied the pattern of the two WASP-positive populations in the different lymphocyte lineages including; CD4+, CD8+, CD20+, CD56+. The results showed that CD20+ cells were $WASP^{low\text{-}bright}$, whereas CD56+ cells were $WASP^{high\text{-}bright}$. In cases of CD4+ and CD8+ cell lineages, both $WASP^{low/high}$ positive peaks were observed. We subsequently studied the pattern of WASP in CD4+/CD45RA+ or CD45RO+ and CD8+/CD45RA+ or CD45RO+ lymphocytes. This demonstrated that CD45RO+ cells that were either CD4+ or CD8+ were $WASP^{high\text{-}bright}$, and that CD45RA+ cells with either CD4+ or CD8+ showed $WASP^{low\text{-}bright}$ (Fig. 2).

Simultaneous staining with two anti-WASP antibodies revealed that the two WASP-positive peaks were detected with 3F3A5, but not with B-9 using

The two lymphocyte WASP-positive peaks observed using FCM-WASP were repeatedly detected using 3F3A5, but not with the B-9 antibody. To clarify these findings, we performed FCM-WASP on normal lymphocytes with simultaneous staining with 3F3A5 and B-9. The results clearly showed that the two WASP-positive peaks could be detected only with 3F3A5, but not with B-9 (Fig. 3A).

No differences in the amount of WASP protein, or WASP mRNA levels were detected between $WASP^{low\text{-}bright}$ and $WASP^{high\text{-}bright}$ cell populations

We isolated the CD3+/CD45RA+ lymphocyte population as $WASP^{low\text{-}bright}$ cells, and CD3+/CD45RO+ population as $WASP^{high\text{-}bright}$ cells. We compared the amount of WASP protein and message levels between these two cell populations. We used WIP as a loading protein control and glyceraldehyde-3-phosphate dehydrogenase as a standard cDNA control. No obvious differences were observed at the WASP protein (Fig. 4A) or message levels (Fig. 4B) between the two populations.

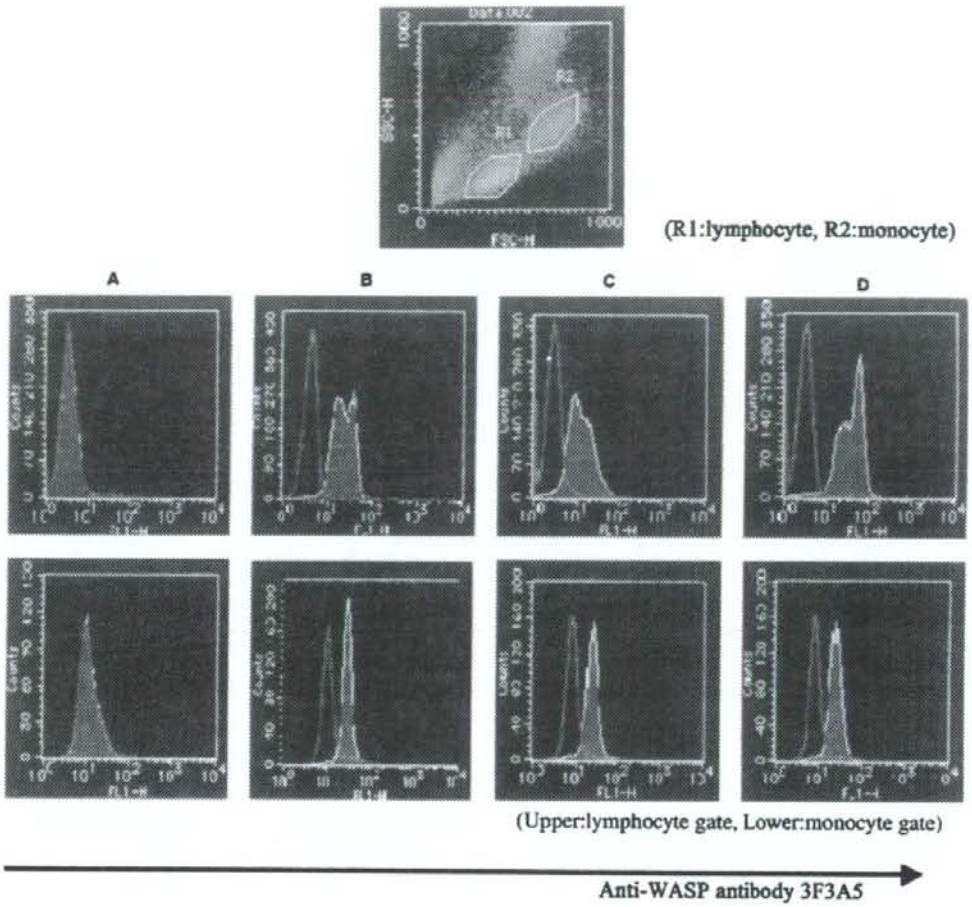

Figure 1 Two WASP-positive populations were detected in lymphocytes by FCM-WASP. Using the anti-WASP antibody 3F3A5, a pattern of two WASP-positive populations; $WASP^{high\text{-}bright}$ cells and $WASP^{low\text{-}bright}$, were observed in lymphocytes from normal individuals. In contrast, monocytes from the same individuals showed only a single WASP-positive population. (A) a patient with WAS, (B–D) normal control individuals. The top figure shows analysis of the lymphocyte gate (R1), and the monocyte gate (R2). The middle 4 figures show the results of lymphocytes, the lower 4 figures show the results of monocytes.

The WASP-positive pattern in CD8+ lymphocytes as seen by FCM-WASP changed during *in vitro* short-term activation

We next studied the effects of short-term lymphocyte activation on the WASP-positive cell pattern by FCM-WASP in the same lineage cells. We used CD8+ lymphocytes, because the CD8+ lineage has two populations most remarkably. To avoid synthesis of new WASP during activation, we settled on using a short-term (4 h) *in vitro* activation system and used 3F3A5 and B-9 antibodies together with FCM-WASP. We purified CD8+ lymphocytes by negative selection and these cells were used for FCM-WASP after PMA/ionomycin stimulation. After the short-term stimulation, the WASP-positive pattern showed significant up-regulation in FCM-WASP using 3F3A5, but not in FCM-WASP using B-9 (Fig. 5).

Discussion

In our previous studies, we noticed that lymphocytes from healthy individuals showed two WASP expression

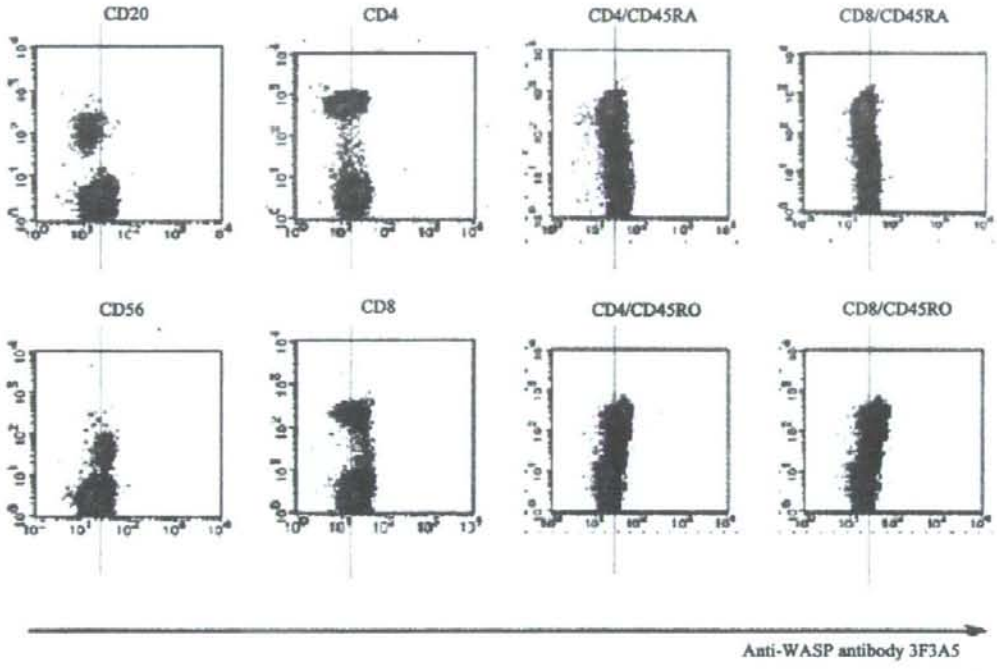

Figure 2 Characterization of the constituent cell lineages of the each WASP-positive population. By dual/triple staining of intracellular WASP and surface cell markers, we determined that CD20+, CD4+/CD45RA+ and CD8+/CD45RA+ cells belonged to the $WASP^{low\text{-}bright}$ population, whereas CD56+, CD4+/CD45RO+ and CD8+/CD45RO+ cells belonged to $WASP^{high\text{-}bright}$.

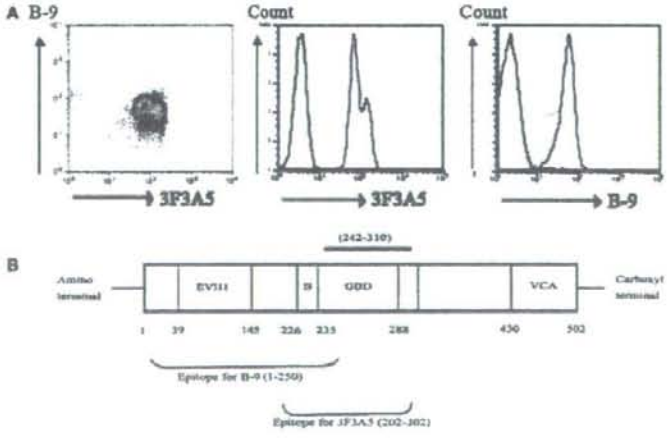

Figure 3 FCM-WASP after simultaneous staining with two different anti-WASP antibodies; 3F3A5 and B-9 (A). The top figure indicates the results of simultaneous analysis with 3F3A5 and B-9, showing two distinct subpopulations using the 3F3A5 antibody, but a single positive population by B-9. The lower two figures show each independent result. The scheme showing the WASP structure (B) Figures indicate amino acid number. The underlined region (242–310) highlights a part of the GBD domain that is thought to be used for binding to the VCA domain in the inactive form of WASP. The scheme includes areas of possible epitopes for B-9 and 3F3A5 antibody binding represented. GBD domain (amino acids 235–288) is included within the 3F3A5 recognition site (amino acids 202–302).

profile populations; $WASP^{low\text{-}bright}$ and $WASP^{high\text{-}bright}$, using FCM-WASP. In this study, we confirmed two WASP-positive cell populations detected in the normal lymphocyte populations using FCM-WASP, and have proposed a possible mechanism causing the two populations.

We characterized the constituent cell lineage members of the each WASP-positive population. It was found that

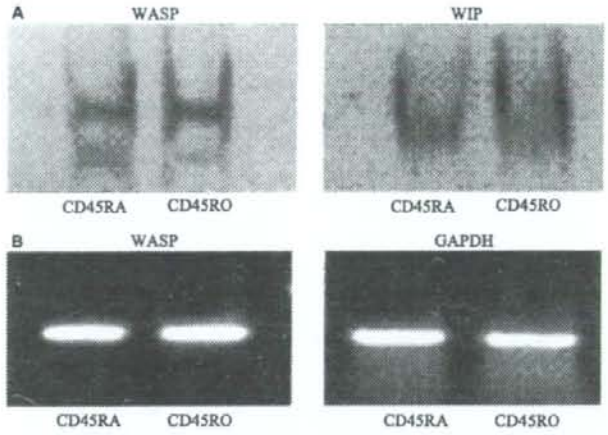

Figure 4 Protein and message levels of WASP in CD3+CD45RA+ cells and CD3+CD45RO+ cells. No significant difference in WASP protein or message levels was observed between WASP$^{low\text{-}bright}$ (CD3+/CD45RA+) and WASP$^{high\text{-}bright}$ (CD3+/CD45RO+) populations. We used WIP as a loading protein control and glyceraldehyde-3-phosphate dehydrogenase (GAPDH) as a standard cDNA control. (A) Western blot analysis. (B) Reverse transcriptase (RT)-PCR analysis

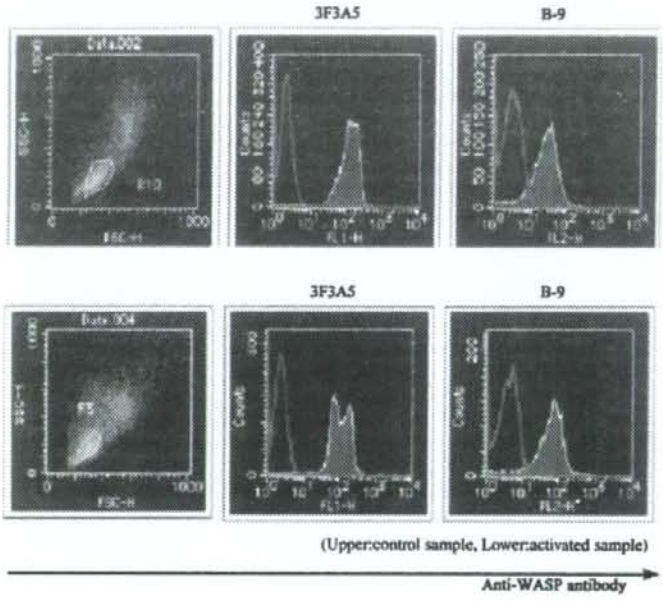

Figure 5 Effects of short-term activation on the WASP expression pattern in CD8+ cells analyzed using FCM-WASP. Purified CD8+ cells were incubated with or without activation for 4 h and the WASP-expression patterns are compared by FCM-WASP. Using the 3F3A5 antibody, the pattern was clearly changed upon activation. In contrast, this postactivation pattern showed no change using B-9.

monocytes, CD20+ cells, CD4+/CD45RA+ cells and CD8+/CD45RA+ cells belonged to the WASP$^{low\text{-}bright}$ population, whereas CD56+ cells, CD4+/CD45RO+ cells and CD8+/CD45RO+ cells belonged to the WASP$^{high\text{-}bright}$ group. It is interesting that these results seem to be linked to the hierarchy of WASP dependency for cell proliferation/survival; which we have proposed based on various aspects of studies on WAS patients and their families. These studies included WAS carrier analysis (21, 22), mixed chimera analysis in WAS patients after hematopoietic stem cell transplantation (25) and cell lineage analysis in WAS patients who showed somatic mosaicism due to spontaneous reversion to normal from inherited mutations (26). Based on these results, we speculated that WASP-dependency was lower in monocytes and B cells compared to T cells, and among T cells, naïve T cells were less WASP dependent than memory T cells. Although we cannot accurately place the requirements for NK cells in this hierarchy for WASP dependency, recent reports suggested that NK cell WASP

dependency seemed high (27, 28). Thus, those less WASP dependent cells belong to the WASP $^{low\text{-}bright}$ population, while highly WASP dependent cells belong to the WASP$^{high\text{-}bright}$ population. This consistency suggests that the difference between the two WASP-positive populations is linked to the difference in the response of these cells through WASP-mediated stimulations.

Next, we studied the basis of differences between the two WASP-positive populations. Differences in WASP staining dot brightness as demonstrated by flow cytometry are generally considered as differences in the quantity of molecules detected by antibodies. Unexpectedly, however, we found that the two WASP-positive lymphocyte populations detected by FCM-WASP were only identified using the 3F3A5 antibody, but not with the B-9 antibody, which was confirmed by simultaneous staining with 3F3A5 and B-9 (Fig. 3A). These results indicate that the difference between WASP$^{low\text{-}bright}$ and WASP$^{high\text{-}bright}$ cells results not from any disparity in WASP expression, but from disparity in antibody binding to WASP that is likely dependant on protein confirmation. Accordingly, we purified CD3+/CD45RA+ and CD3+/CD45RO+ cells, representing WASP$^{low\text{-}bright}$ and WASP$^{high\text{-}bright}$ populations respectively, and performed Western blot and RT-PCR analysis. The results showed there was no apparent difference in WASP or *WASP* mRNA levels between them (Fig. 4A,B), supporting the speculation that there is no disparity in WASP expression between lymphocytes showing WASP$^{low\text{-}bright}$ and WASP$^{high\text{-}bright}$ staining patterns.

Recently, WASP autoinhibition and activation mechanisms have been reported (10). The crystal structure model of the WASP, indicated that it could exist in either an activated or an inactivated form based on intramolecular structural changes. WASP has an N-terminal Ena/VASP homology domain 1 (EVH1) domain, a Cdc42/Rac GTPase binding domain (GBD), a proline-rich domain, a G-actin binding verprolin homology (V) domain, a cofilin homology (C) domain and a C-terminal acidic (A) segment.

WASP interacts with Cdc42-GTP via its GBD, with multiple SH3 domain-containing proteins that include Nck via its proline-rich region, with actin and the ARP2/3 complex via its VCA domain. WASP is usually present in cells in a closed, inactive conformation due to intramolecular regulatory interactions that involve the C-terminal acidic domain and the basic region that precedes the GBD. Binding of Cdc42-GTP is thought to cause WASP conformational change, which allows the VCA domain to interact with and activate the Arp2/3 complex (10) (Fig. 3B).

Based on these auto-inactivation and activation mechanisms of WASP, we speculate that the results from the two WASP-positive lymphocyte populations detected by FCM-WASP are related to this mechanism. As shown in Fig. 4, the two WASP-positive lymphocyte populations were detected with anti-WASP antibody 3F3A5, not with B-9. The WASP epitopes recognized by these two antibodies are different; 3F3A5 recognizes an epitope within amino acids 202~302 of WASP (this region includes the GBD), whereas the B-9 antibody recognizes an epitope lying within 1~250 amino acids of WASP (11). It is important to note that a part of the GBD (amino acids 235~288), that is hypothesized to be involved in binding to the VCA domain in the inactive form of WASP, might be included in the 3F3A5 antibody recognition site. Thus, we propose that the 3F3A5 antibody might be able to be used to distinguish a structural or activation state change in WASP, that is not possible using the B-9 antibody.

Finally, we studied the effects of short-term activation on the WASP-positive pattern by FCM-WASP in these CD8+ lineage cells. To avoid new WASP synthesis, we cultured cells for short term *in vitro* activation (4 h). Our data revealed that short-term activation forced a dramatic change to the WASP$^{high\text{-}bright}$ pattern in the same cell lineage (Fig. 5).

Here we report a new possible application of flow cytometry for analysis of intracellular WAS protein and its structural and functional status. However, from our data we cannot determine the relation or possible function of the two WASP-positive populations and their relationship to their WASP activation or inactivation status. Further different aspects of studies, such as FCM-WASP for patients with XLN, will be needed to answer these questions.

Acknowledgements

This study was supported by Grant-in-aid for Scientific Research from the Japanese Ministry of Health, Labor and Welfare (2542002917, 15COE011-02 and H19-Child-General-003).

References

1. Stewart DM, Tian L, Nelson DL. Mutations that cause the Wiskott-Aldrich syndrome impair the interaction of Wiskott-Aldrich syndrome protein (WASP) with WASP interacting protein. *J Immunol* 1999;**162**:5019–24.
2. Derry JMJ, Ochs HD, Francke U. Isolation of a novel gene mutated in Wiskott-Aldrich syndrome. *Cell* 1994;**78**:635–44.
3. Symons M, Derry JMJ, Karlak B, Jiang S, Lemahieu V, Mccormick F, Francke U, Abo A. Wiskott-Aldrich syndrome protein, a novel effector for the GTPase CDC42Hs, is implicated in actin polymerization. *Cell* 1996;**84**:723–34.

4. Molina IJ, Sancho J, Terhorst C, Rosen FS, Remold-O'Donnell E. T cells of patients with the Wiskott-Aldrich syndrome have a restricted defect in proliferative responses. *J Immunol* 1993;**151**:4383–90.
5. Cory GOC, MacCarthy-Morrogh L, Banin S, Gout I, Brickell PM, Levinsky RI, Kinnon C, Lovering RC. Evidence that the Wiskott-Aldrich syndrome protein may be involved in lymphoid cell signaling pathways. *J Immunol* 1996;**157**:3791–5.
6. Rudolph MG, Bayer P, Abo A, Kuhlmann J, Vetter IR, Wittinghofer A. The CDC42/Racinteractive binding region motif of the Wiskott-Aldrich syndrome protein (WASP) is necessary but not sufficient for tight binding to CDC42 and structure formation. *J Biol Chem* 1998;**273**:18067–76.
7. Higgs HN, Pollard TD. Regulation of actin filament network formation through arp2/3 complex: activation by a diverse array of proteins. *Annu Rev Biochem* 2001;**70**:649–76.
8. Gallego MD, Santamaria M, Pena J, Molina IJ. Defective actin reorganization and polymerization of Wiskott-Aldrich syndrome T cells in response to CD3-mediated stimulation. *Blood* 1997;**90**:3089–97.
9. Candotti F, Facchetti F, Blanzuoli L, Stewart DM, Nelson DL, Blaese RM. Retrovirus-mediated WASP gene transfer corrects defective actin polymerization in cell lines from Wiskott-Aldrich syndrome patients carrying null mutations. *Gene Ther* 1999;**6**:1170–4.
10. Kim AS, Kakalis LT, Abdul-Manan N, Liu GA, Rosen MK. Autoinhibition and activation mechanism of the Wiskott-Aldrich syndrome protein. *Nature* 2000;**404**:151–8.
11. Stewart DM, Treiber-Held S, Kurman CC, Facchetti F, Notarangelo LD, Nelson DL. Studies of the expression of the Wiskott-Aldrich syndrome protein. *J Clin Invest* 1996;**97**:2627–34.
12. Derry JMJ, Kerns JA, Weinberg KI, Ochs HD, Volpini V, Estivill X, Walker AP, Franke U. WASP gene mutations in Wiskott-Aldrich syndrome and X-linked thrombocytopenia. *Hum Mol Genet* 1995;**4**:1127–35.
13. Devriendt K, Kim AS, Mathijs G, *et al.* Constitutively activating mutation in WASP causes X-linked severe congenital neutropenia. *Nat Genet* 2001;**27**:313–7.
14. Aldrich RA, Steinber AG, Campbell DC. Pedigree demonstrating a sex-linked recessive condition characterized by draining ears, eczematoid dermatitis and bloody diarrhea. *Pediatrics*. 1954;**13**:133–9.
15. Sullivan KE, Mullen CA, Blaese RM, Winkeistein JA. A multi-institutional survey of the Wiskott-Aldrich syndrome. *J Pediatr* 1994;**125**:876–85.
16. Ochs HD. The Wiskott-Aldrich syndrome. *Semin Hematol* 1998;**35**:332–45.
17. Oda A, Ochs HD. Wiskott-Aldrich syndrome protein and platelets. *Immunol Rev* 2000;**178**:111–7.
18. Lutskiy MI, Rosen FS, Remold-O'Donnell E. Genotype-proteotype linkage in the Wiskott-Aldrich syndrome. *J Immunol* 2005;**175**:1329–36.
19. Folwaczny C, Ruelfs C, Walther J, König A, Emmerich B. Ulcerative colitis in a patient with Wiskott-Aldrich syndrome. *Endoscopy* 2005;**34**:840–1.
20. Johnston SL, Unsworth DJ, Dwight JF, Kennedy CTC. Wiskott-Aldrich syndrome, vasculitis and critical aortic dilatation. *Acta Paediatr* 2002;**90**:1346–8.
21. Yamada M, Ohtsu M, Kobayashi I, *et al.* Flow cytometric analysis of Wiskott-Aldrich syndrome (WAS) protein in lymphocytes from WAS patients and their familial carriers. *Blood* 1999;**93**:756–62.
22. Yamada M, Ariga T, Kawamura N, *et al.* Determination of carrier status for the Wiskott-Aldrich syndrome by flow cytometric analysis of Wiskott-Aldrich protein expression in peripheral blood mononuclear cells. *J Immunol* 2000;**165**:1119–22.
23. Ariga T, Yamada M, Wada T, Saitoh S, Sakiyama Y. Detection of lymphocytes and granulocytes expressing the mutant WASP message in carriers of Wiskott-Aldrich syndrome. *Br J Haematol* 1999;**104**:893–900.
24. Ariga T, Yamada M, Sakiyama Y. Mutation analysis of five Japanese families with Wiskott-Aldrich syndrome and determination of the family members'carrier status using three different methods. *Pediatr Res* 1997;**41**:535–40.
25. Yamaguchi K, Ariga T, Yamada M, *et al.* Mixed chimera status of 12 patient with Wiskott-Aldrich syndrome (WAS) after hematopoietic stem cell transplantation; evaluation by flow cytometric analysis of intracellular WAS protein expression. *Blood* 2002;**100**:1208–14.
26. Ariga T, Kondoh T, Yamaguchi K, Yamada M, Sasaki S, Nelson DL, Ikeda H, Kobayashi K, Moriuchi H, Sakiyama Y. Spontaneous in vivo reversion of an inherited mutation in the Wiskott-Aldrich syndrome. *J Immunol* 2001;**166**:5245–9.
27. Lutskiy MI, Beardsley DS, Rosen FS, Remold-O'Donnell E. Mosaicism of NK cells in a patient with Wiskott-Aldrich syndrome. *Blood* 2005;**106**:2815–7.
28. Orange JS, Ramesh N, Remold-O'Donnell E, Sasahara Y, Koopman L, Byrne M, Bonilla FA, Rosen FS, Geha RS, Strominger JL. Wiskott-Aldrich syndrome protein is required for NK cell cytotoxicity and colocalizes with actin to NK cell-activating immunologic synapses. *Proc Natl Acad Sci USA* 2002;**99**:11351–6.

Bone Marrow Transplantation (2008) 42, 743–748

www.nature.com/bmt

ORIGINAL ARTICLE

The syndrome of inappropriate secretion of antidiuretic hormone associated with SCT: clinical differences following SCT using cord blood and BM/peripheral blood

Y Suzuki[1,2], R Kobayashi[3], A Iguchi[4], T Sato[3], M Kaneda[2], K Kobayashi[2,3] and T Ariga[2]

[1]*Department of Pediatrics, Oji General Hospital, Hokkaido, Japan;* [2]*Department of Pediatrics, Hokkaido University Graduate School of Medicine, Hokkaido, Japan;* [3]*Department of Pediatrics, Sapporo Hokuyu Hospital, Hokkaido, Japan and* [4]*Department of Pediatrics, Asahikawa Medical College School of Medicine, Hokkaido, Japan*

Previously, we reported the syndrome of inappropriate secretion of antidiuretic hormone (SIADH) as an underestimated complication associated with SCT. In the present report, we analyzed detailed data on a larger number of patients with SIADH following SCT and found different SIADH clinical features following cord blood SCT (CBSCT) and BMT/PBSCT. The median onset of SIADH following CBSCT and BMT/PBSCT was 19 and 46 days after SCT, respectively, and the median numbers of WBC at the onset of SIADH were 1.0 and 3.1 $\times 10^9$/l, respectively. Furthermore, severe symptoms such as seizures, somnolence and rigidity of limbs were observed only in patients with CBSCT (8/15 *vs* 0/10). These differences were statistically significant ($P<0.01$). Although the precise basis for SIADH following SCT still remains unknown, the different features of SIADH observed following CBSCT and BMT/PBSCT may provide important clues to the disease mechanism following SCT. Additionally, we confirmed our previous results that patients with SIADH showed a higher overall survival and event-free survival rates. However, we first suggested that they had some neurological disorders and that neurological sequelae such as developmental delay and seizures would consequently occur.

Bone Marrow Transplantation (2008) **42,** 743–748; doi:10.1038/bmt.2008.247; published online 18 August 2008
Keywords: syndrome of inappropriate secretion of antidiuretic hormone; SCT; cord blood SCT; neurological sequelae

Introduction

Hematopoietic SCT has been an approved treatment for hematological diseases (for example, leukemia, lymphoma and aplastic anemia), certain solid organ tumors, immunodeficiencies, metabolic diseases, among other disorders. However, SCT can cause many complications, such as GVHD, opportunistic infections and graft failure. Although the syndrome of inappropriate secretion of antidiuretic hormone (SIADH) also seems to be one of these complications, there are only few case reports available on SIADH following SCT,[1,2] including our previous report.[3] Therefore, SIADH following SCT has had its importance underestimated.

In our previous report,[3] severe hyponatremia of less than 125 mmol/l was a complication in 27 (19.3%) of the 140 SCT patients, and 16 (56.9%) of them were diagnosed with SIADH. Moreover, multivariate analysis revealed that alternative donor and recipient below the age of 4 years were the only independent predictors of SIADH. However, the mechanism causing SIADH following SCT and the clinical characteristics are still poorly understood. Thus, in this report, we analyzed detailed data on a larger number of patients with SIADH following SCT.

Patients and methods

This study comprised 197 consecutive pediatric patients (126 boys and 71 girls) who received SCT for malignant (149 patients) or non-malignant disease (48 patients) at the Department of Pediatrics, Hokkaido University Hospital between February 1988 and March 2007. Of these patients, 164 received allogeneic transplantation and the remaining 33 patients received autologous transplantation. As prophylaxis for GVHD, almost all patients receiving BMT/PBSCT received CsA or tacrolimus (FK506) with MTX, whereas almost all patients undergoing cord blood SCT (CBSCT) received CsA with methylprednisolone. CsA and FK506 doses were appropriately adjusted to maintain trough levels of 150–200 ng/ml and 10–20 ng/ml, respectively. All patients received antifungal prophylaxis with amphotericin B or micafungin, antiherpes simplex virus prophylaxis with acyclovir and gut sterilization with polymixin B. Moreover, i.v. immunoglobulin and G-CSF were administered to all patients during the peritransplant

Correspondence: Dr Y Suzuki, Department of Pediatrics, Oji General Hospital, 3-4-8 Wakakusa, Tomakomai, Hokkaido 053-8506, Japan.
E-mail: yoshisuzu_mail@yahoo.co.jp
Received 8 January 2008; revised 24 June 2008; accepted 27 June 2008; published online 18 August 2008

period. Transplant characteristics of all patients are summarized in Table 1.

Serum sodium levels were measured in every patient by a routine automated analyzer every morning until 40 days after SCT and two to three times a week afterwards. We defined hyponatremia as a serum sodium level of less than 125 mmol/l on two consecutive days because serum sodium levels transiently between 125 and 135 mmol/l may not be clinically important. SIADH was diagnosed using the approach reported by Bartter and Schwartz.[4] Diagnosis requires the presence of all of the following criteria: (1) hyponatremia with hypotonicity of plasma; (2) urine osmolality in excess of plasma osmolality; (3) increased renal sodium excretion; (4) absence of edema or volume depletion and (5) normal renal and adrenal function.

A *t*-test or a χ^2 test was used to compare patients with CBSCT and BMT/PBSCT. Statistical analyses were performed using SPSS II for Windows (release 11.0.1J, SPSS Japan Inc.). A *P*-value of less than 0.05 was regarded as statistically significant.

Table 1 Transplant characteristics of all patients

	No. of patients
Disease	
Neoplastic	
ALL	62
First CR	30
Second CR	21
Third or later CR	11
AML	33
First CR	17
Second CR	11
Third or later CR	4
Not CR	1
Neuroblastoma	12
Non-Hodgkin's lymphoma	10
Myelodysplastic syndrome	8
Juvenile myelomonocytic leukemia	8
Rhabdomyosarcoma	7
CML	6
Yolk sac tumor	1
Hepatoblastoma	1
Primitive neuroectodermal tumor	1
Non-neoplastic	
Aplastic anemia	29
Wiskott–Aldrich syndrome	5
SCID	3
Kostmann syndrome	3
Hurler syndrome	2
Chronic granulomatous disease	2
Hunter syndrome	1
X-linked hyper IgM syndrome	1
Chronic active EBV infection	1
Hurler–Scheie syndrome	1
Donor	
Matched related	62
Mismatched related	16
Matched unrelated	48
Mismatched unrelated	38
Autologous	33
Source of stem cells	
BM	122
PB	25
BM + PB	4
Cord blood	46
Conditioning regimen	
TBI	93
BU	69
Melphalan (L-PAM)	57
CY	125
Etoposide (VP16)	93
Antithymocyte globulin	43
Acute GVHD (>2)	33
GVHD prophylaxis	
CsA	119
MTX	113
Tacrolimus (FK506)	33
Methylprednisolone	44

Results

Syndrome of inappropriate secretion of antidiuretic hormone developed in 25 (12.7%) of the 197 patients who received SCT, and a summary of the backgrounds of the patients with SIADH is provided in Table 2. They included 17 boys and 8 girls, ranging from 0 to 15 years old. Of them, 15 received CBSCT, 9 received BMT and 1 received PBSCT. No patient receiving autologous transplantation developed SIADH. Donors were HLA-mismatched unrelated (13 patients), HLA-matched unrelated (6), HLA-mismatched related (5) and HLA-matched related (1). In other words, 24 (96.0%) of the 25 patients with SIADH had received SCT from alternative donors. The symptoms of SIADH were nausea (15 patients), seizure (5), somnolence (2) and rigidity of limbs (1), but two patients exhibited no symptoms. The median of minimum serum sodium level was 120 mmol/l. The median onset of SIADH was 27 days after SCT and the median number of WBC at the onset of SIADH was 2.3×10^9/l.

Neurological sequelae such as developmental delay and seizure occurred in 5 (20.0%) of the 25 patients with SIADH, whereas in 2 (1.2%) of the 172 patients without SIADH ($P<0.01$). All patients with neurological sequelae had received allogeneic transplantation. In analysis limited to survivors, neurological sequelae occurred in 5 (23.8%) of the 21 survivors with SIADH, but they occurred in 2 (2.1%) of the 94 survivors without SIADH ($P<0.01$).

In the patients with SIADH, we compared the above-mentioned factors between patients after CBSCT and those after BMT/PBSCT (Table 3). Age, gender and minimum serum sodium level did not differ between them. However, severe symptoms such as seizure, somnolence and rigidity of limbs were observed in 8 (53.3%) of the 15 patients with CBSCT, but in none of the 10 patients with BMT/PBSCT ($P<0.01$). Additionally, SIADH developed earlier in patients receiving CBSCT (median onset, 19 days after SCT; range, 15–54 days) than in those receiving BMT/PBSCT (median onset, 46 days after SCT; range, 18–74 days), and the median numbers of WBC at the onset of SIADH were lower in patients after CBSCT (median, 1.0×10^9/l; range, $0.1–4.2 \times 10^9$/l) than in those after BMT/PBSCT (median, 3.1×10^9/l; range, $2.5–13.3 \times 10^9$/l) (Figure 1). These differences were statistically significant ($P<0.01$).

Table 2 Profile of patients with SIADH

No.	Age (years)	Gender	SCT	HLA mismatch	Disease	Conditioning regimen	GVHD prophylaxis	At the time of SIADH				Neurological sequelae
								Na (mmol/l)	Day	WBC ($\times 10^8$/l)	Symptom	
1	4	M	U-BMT	0	JMML (CP)	TBI + VP16 + CY	CsA + short MTX	122	40	2.8	Nausea	Dead
2	10	M	R-BMT	1	AML (CR1)	TBI + VP16 + CY + ATG	CsA + short MTX	121	60	2.5	Nausea	None
3	1	M	U-CBSCT	0	WAS	BU + CY	CsA + short MTX	110	32	1.6	Seizure	None
4	7	F	U-CBSCT	1	AML (CR2)	BU + L-PAM	CsA + mPSL	118	41	4.2	None	Dead
5	1	M	U-CBSCT	1	NHL (CR3)	TBI + VP16 + CY	CsA + mPSL	120	15	1.0	Nausea	DD, seizure
6	5	F	U-CBSCT	1	AML (CR2)	BU + L-PAM	CsA + mPSL	121	18	1.0	Nausea	None
7	1	M	R-BMT	1	Aplastic anemia	TLI + ATG + CY	CsA + short MTX	106	74	3.3	Nausea	None
8	3	F	U-BMT	0	Aplastic anemia	TBI + ATG + CY	FK506 + short MTX	115	27	4.2	Nausea	None
9	7	F	R-PBSCT	1	ALL (CR1)	ATG + CY	FK506 + short MTX	115	54	0.2	Nausea	None
10	3	M	R-BMT	0	ALL (CR1)	TBI + VP16 + CY	CsA + short MTX	121	52	2.9	Nausea	None
11	9	F	U-CBSCT	2	NB (CR1)	CBDCA + VP16 + L-PAM	CsA + mPSL	117	19	0.1	Nausea	None
12	0	M	U-CBSCT	0	WAS	BU + CY + ATG	CsA + mPSL	122	19	0.9	Nausea	None
13	10	F	U-BMT	0	ALL (CR1)	TBI + VP16 + CY	FK506 + short MTX	123	31	6.4	Nausea	None
14	12	M	R-BMT	1	AML (CR2)	BU + L-PAM	FK506 + short MTX	122	18	13.3	Nausea	Dead
15	2	M	R-BMT	1	Hurler Scheie	BU + CY + ATG	FK506 + short MTX	123	35	2.7	Nausea	None
16	3	M	U-CBSCT	1	JMML (CP)	TBI + Ara-C + CY	CsA + mPSL	123	34	0.6	Seizure	Dead
17	6	M	U-CBSCT	1	ALL (CR2)	TBI + VP16 + CY	CsA + mPSL	115	28	0.5	Somnolence	DD, seizure
18	14	F	U-CBSCT	2	CAEBV	Flu + VP16 + TBI	CsA + mPSL	118	22	1.6	Seizure	Seizure
19	11	F	U-CBSCT	1	ALL (CR1)	TBI + VP16 + CY	CsA + mPSL	117	15	1.2	Somnolence	None
20	7	M	U-CBSCT	1	ALL (non-CR)	TBI + VP16 + CY	CsA + mPSL	120	17	2.4	Nausea	None
21	4	M	U-CBSCT	1	Aplastic anemia	Flu + L-PAM + TBI	CsA + mPSL	120	20	0.4	Seizure	DD, seizure
22	5	M	U-CBSCT	1	AML (CR3)	BU + L-PAM	CsA + mPSL	120	15	2.5	Rigidity of limbs	None
23	3	M	U-CBSCT	1	NB (CR1)	TBI + VP16 + CY	CsA + mPSL	115	17	0.2	Seizure	None
24	15	M	U-BMT	1	ALL (CR3)	BU + L-PAM	FK506 + short MTX	122	72	5.6	Nausea	Seizure
25	11	M	U-CBSCT	2	ALL (CR3)	TBI + VP16 + CY	CsA + mPSL	123	21	2.3	None	None

Abbreviations: Ara-C = cytarabine; ATG = antithymocyte globulin; CAEBV = chronic active EBV infection; CBDCA = carboplatine; CBSCT = cord blood SCT; DD = developmental delay; FK506 = tacrolimus; Flu = fludarabine; JMML = juvenile myelomonocytic leukemia; L-PAM = melphalan; mPSL = methyl prednisolone; Na = sodium; NB = neuroblastoma; NHL = non-Hodgkin's lymphoma; TLI = total lymphoid irradiation; SIADH = syndrome of inappropriate antidiuretic hormone; VP16 = etoposide; WAS = Wiskott–Aldrich syndrome.

Table 3 Comparison between patients with CBSCT and BMT/PBSCT

	CBSCT (n = 15)	*BMT/PBSCT (n = 10)*
Gender		
Male	10	7
Female	5	3
Age (median, years old)	5	6
Minimum sodium level (median, mmol/l)	120	121.5
Onset of SIADH (median, day)	19*	46*
WBC at onset of SIADH (median, $\times 10^9$/l)	1.0*	3.1*
Severe symptom at SIADH	8*	0*
Neurological sequelae	4	1

Abbreviations: CBSCT = cord blood SCT; SIADH = syndrome of inappropriate antidiuretic hormone.
*$P < 0.05$.

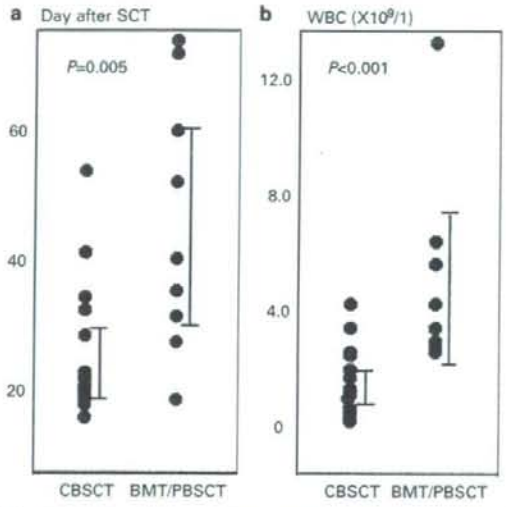

Figure 1 (a) Day of the onset of syndrome of inappropriate secretion of antidiuretic hormone (SIADH) following cord blood SCT (CBSCT) and BMT/PBSCT. (b) WBC at the onset of SIADH in patients with CBSCT and BMT/PBSCT.

Neurological sequelae occurred in 4 (26.6%) of the 15 patients receiving CBSCT, but in only 1 (10.0%) of the 10 patients after BMT/PBSCT. In analysis limited to survivors, neurological sequelae occurred in 4 (30.8%) of the 13 survivors after CBSCT, whereas it occurred in one (12.5%) of the eight survivors following BMT/PBSCT. These differences were not significant ($P > 0.30$).

Discussion

In this study, we revealed for the first time the differences in SIADH clinical features between CBSCT and BMT/PBSCT treatments; patients receiving CBSCT had an earlier onset, a lower WBC count at the onset, and more severe symptoms than did those receiving BMT/PBSCT, and neurological sequelae were more frequent following SCT in survivors with SIADH than in those without SIADH.

Antineoplastic agents,[5,6] glucocorticoid,[7] hematological diseases[8–11] and other factors have been reported to be associated with SIADH. In this study, multivariate analysis revealed that only an alternative donor was independently associated with an increased risk of SIADH, whereas recipient age, gender, primary diseases, acute GVHD or drugs used in the peritransplant period were not independent risk factors (data not shown). These results, except for age, concurred with our previous report.[3] Although we have no available data at present, IL-6 has been reported to be involved in SIADH.[12–14] In addition, levels of cytokines such as IL-6 and tumor necrosis factor-α are known to be high in SCT from an HLA-mismatched donor or an unrelated donor.[15] These cytokines may induce SIADH following SCT, even though acute GVHD was not associated with the occurrence of SIADH.

In patients with SIADH following SCT, we found different SIADH clinical features following CBSCT and BMT/PBSCT. CsA and methylprednisolone were used more frequently in patients with SIADH following CBSCT, whereas antithymocyte globulin, FK506 and MTX were used more frequently in patients with SIADH following BMT/PBSCT ($P < 0.04$). These drugs, however, were not associated with the occurrence of SIADH. Therefore, these clinical differences are likely due to the difference in the source of stem cells. A major difference in the outcome between CBSCT and BMT/PBSCT is recognized to be that CBSCT needs a longer period for hematological/immunological reconstitution than does BMT/PBSCT. However, the hypothesis that SIADH following SCT treatment is related to the expansion of donor cells is not likely because patients with SIADH following CBSCT had an approximate 3 week earlier onset and one-third of the WBC count at the onset compared to those with SIADH following BMT/PBSCT. The difference in cytokine reactions between CBSCT and BMT/PBSCT, such as pre-engraftment immune reactions proposed as an early phenotype of post-CBSCT immune reaction,[16,17] may explain these clinical differences.

We have previously shown significantly higher overall and event-free survival rates in patients with SIADH following SCT than those without SIADH.[3] In this study, although this conclusion was confirmed (data not shown), neurological sequelae following SCT occurred in survivors with SIADH more frequently than in those without SIADH. All patients with SIADH were promptly and appropriately treated with fluid restriction, diuretics or hypertonic saline (3% NaCl) and recovered from hyponatremia. NaCl (3%) was given to 23 of the 25 patients and its duration (median, 23 days; range, 1–116 days) was not associated with the source of stem cells or neurological sequelae (data not shown). Patients had no other metabolic disturbances, such as hypocalcaemia, hypomagnesaemia and hyper- or hypoglycemia. Only one patient diagnosed with human herpes virus 6 (HHV-6) encephalitis had a

neurological disorder other than SIADH. We therefore speculate that the causes of neurological sequelae are identical to those of SIADH. Although the precise basis for SIADH following SCT still remains unknown, there may be a pattern of cytokines inducing not only SIADH but also a GVL/tumor effect without GVHD. To test this hypothesis, it is important to determine whether there are significant differences in survival rates between malignant and non-malignant diseases. For this purpose, further analysis of a much larger number of patients with SIADH following SCT will be needed.

After the onset of SIADH, one patient (case 21) was diagnosed with HHV-6 encephalitis by PCR for HHV-6 using his cerebrospinal fluid. Although he was appropriately treated for SIADH and recovered from hyponatremia, he finally subsequently developed seizures and developmental delay. There are also a few reports of SIADH related to HHV-6 encephalitis.[18,19] Therefore, we speculate that, in this case, HHV-6 encephalitis caused SIADH and neurological sequelae. SCT often causes many neurological disorders,[20–22] some of which, such as CNS infections (bacterial and viral),[18,19,23–26] intracranial bleeding and drug toxicity (FK506),[27] have been reported to be associated with SIADH. Thus, subclinical neurological disorders might be present in these patients and elude diagnosis, although we were unable to demonstrate any neurological disorders in other patients with SIADH. Not only cytokine reactions after SCT but also neurological disorders caused by SCT can cause SIADH following SCT and neurological sequelae. SIADH may be considered as a potentially important symptom of neurological disorders and a predictor of neurological sequelae.

In conclusion, we revealed the differences in SIADH clinical features between CBSCT and BMT/PBSCT treatments and the more frequent occurrence of neurological sequelae following SCT in survivors with than without SIADH. The onset of SIADH following SCT was assumed to be associated with cytokine reactions after SCT and/or other neurological disorders caused by SCT. Further analysis of a much larger number of patients with SIADH following SCT is needed to explore the mechanisms of SIADH developing after SCT and to appropriately manage such patients.

References

1 Abe T, Takaue Y, Okamoto Y, Yamaue T, Nakagawa R, Makimoto A *et al.* Syndrome of inappropriate antidiuretic hormone secretion (SIADH) in children undergoing high-dose chemotherapy and autologous peripheral blood stem cell transplantation. *Pediatr Hematol Oncol* 1995; **12**: 363–369.
2 Festuccia F, Polci R, Pugliese F, Gargiulo A, Cinotti GA, Menè P. Syndrome of inappropriate ADH secretion: a late complication of hemopoietic stem cell allograft. *G Ital Nefrol* 2002; **19**: 353–360.
3 Kobayashi R, Iguchi A, Nakajima M, Sato T, Yoshida M, Kaneda M *et al.* Hyponatremia and syndrome of inappropriate antidiuretic hormone secretion complicating stem cell transplantation. *Bone Marrow Transplant* 2004; **34**: 975–979.
4 Bartter FC, Schwartz WB. The syndrome of inappropriate secretion of antidiuretic hormone. *Am J Med* 1967; **42**: 790–806.
5 Sorensen JB, Andersen MK, Hansen HH. Syndrome of inappropriate secretion of antidiuretic hormone (SIADH) in malignant disease. *J Intern Med* 1995; **238**: 97–110.
6 Sica S, Cicconi S, Sorà F, Chiusolo P, Piccirillo N, Laurenti L *et al.* Inappropriate antidiuretic hormone secretion after high-dose thiotepa. *Bone Marrow Transplant* 1999; **24**: 571–572.
7 Liu RY, Unmehopa UA, Zhou JN, Swaab DF. Glucocorticoids suppress vasopressin gene expression in human suprachiasmatic nucleus. *J Steroid Biochem Mol Biol* 2006; **98**: 248–253.
8 Chubachi A, Miura I, Hatano Y, Ohshima A, Nishinari T, Miura AB. Syndrome of appropriate secretion of antidiuretic hormone in patients with lymphoma associated hemophagocytic syndrome. *Ann Hematol* 1995; **70**: 53–55.
9 Ciaudo M, Chauvenet L, Audouin J, Rossert J, Favier R, Horellou MH *et al.* Peripheral T-cell lymphoma with hemophagocytic histiocytosis localized to the bone marrow associated with inappropriate secretion of antidiuretic hormone. *Leukemia Lymphoma* 1995; **19**: 511–514.
10 Eliakim R, Vertman E, Shinhar E. Syndrome of inappropriate secretion of antidiuretic hormone in Hodgkin's disease. *Am J Med Sci* 1986; **291**: 126–127.
11 Kelton JG, Logue G. Inappropriate antidiuretic hormone complicating histiocytic lymphoma. *Arch Intern Med* 1979; **139**: 307–308.
12 Mastorakos G, Weber JS, Magiakou MA, Gunn H, Chrousos GP. Hypothalamic-pituitary-adrenal axis activation and stimulation of systemic vasopressin secretion by recombinant interleukin-6 in humans: potential implications for the syndrome of inappropriate vasopressin secretion. *J Clin Endocrinol Metab* 1994; **79**: 934–939.
13 Gionis D, Ilias I, Moustaki M, Mantzos E, Papadatos I, Koutras DA *et al.* Hypothalamic-pituitary-adrenal axis and interleukin-6 activity in children with head trauma and syndrome of inappropriate secretion of antidiuretic hormone. *J Pediatr Endocrinol Metab* 2003; **16**: 49–54.
14 Ghorbel MT, Sharman G, Leroux M, Barrett T, Donovan DM, Becker KG *et al.* Microarray analysis reveals interleukin-6 as a novel secretory product of the hypothalamo-neurohypophyseal system. *J Biol Chem* 2003; **278**: 19280–19285.
15 Nagler A, Bishara A, Brautbar C, Barak V. Dysregulation of inflammatory cytokines in unrelated bone marrow transplantation. *Cytokines Cell Mol Ther* 1998; **4**: 161–167.
16 Kishi Y, Kami M, Miyakoshi S, Kanda Y, Murashige N, Teshima T *et al.* Early immune reaction after reduced-intensity cord-blood transplantation for adult patients. *Transplantation* 2005; **80**: 34–40.
17 Narimatsu H, Terakura S, Matsuo K, Oba T, Uchida T, Iida H *et al.* Short-term methotrexate could reduce early immune reactions and improve outcomes in umbilical cord blood transplantation for adults. *Bone Marrow Transplant* 2007; **39**: 31–39.
18 Shimura N, Kim H, Sugimoto H, Aoyagi Y, Baba H, Kim S. Syndrome of inappropriate secretion of antidiuretic hormone as a complication of human herpesvirus-6 infection. *Pediatr Int* 2004; **46**: 497–498.
19 Okafuji T, Uchiyama H, Okabe N, Akatsuka J, Maekawa K. Syndrome of inappropriate secretion of antidiuretic hormone associated with exanthem subitum. *Pediatr Infect Dis J* 1997; **16**: 532–533.
20 de Brabander C, Cornelissen J, Smitt PA, Vecht CJ, van den Bent MJ. Increased incidence of neurological complications in patients receiving an allogenic bone marrow transplantation

from alternative donors. *J Neurol Neurosurg Psychiatry* 2000; **68**: 36–40.

21 Bleggi-Torres LF, de Medeiros BC, Werner B, Neto JZ, Loddo G, Pasquini R *et al.* Neuropathological findings after bone marrow transplantation: an autopsy study of 180 cases. *Bone Marrow Transplant* 2000; **25**: 301–307.

22 Weber C, Schaper J, Tibussek D, Adams O, MacKenzie CR, Dilloo D *et al.* Diagnostic and therapeutic implications of neurological complications following paediatric haematopoietic stem cell transplantation. *Bone Marrow Transplant* 2008; **41**: 253–259.

23 Drakos P, Weinberger M, Delukina M, Or R, Nagler A, Weinberg M. Inappropriate antidiuretic hormone secretion (SIADH) preceding skin manifestations of disseminated varicella zoster virus infection. *Bone Marrow Transplant* 1993; **11**: 407–408.

24 Szabó F, Horvath N, Seimon S, Hughes T. Inappropriate antidiuretic hormone secretion, abdominal pain and disseminated varicella-zoster virus infection: an unusual triad in a patient 6 months post mini-allogeneic peripheral stem cell transplant for chronic myeloid leukemia. *Bone Marrow Transplant* 2000; **26**: 231–233.

25 Sato H, Kamoi K, Saeki T, Yamazaki H, Koike T, Miyamura S *et al.* Syndrome of inappropriate secretion of antidiuretic hormone and thrombocytopenia caused by cytomegalovirus infection in a young immunocompetent woman. *Intern Med* 2004; **43**: 1177–1182.

26 Nagamitsu S, Okabayashi S, Dai S, Morimitsu Y, Murakami T, Matsuishi T *et al.* Neuroimaging and neuropathologic findings in AIDS patient with cytomegalovirus infection. *Intern Med* 1994; **33**: 158–162.

27 Azuma T, Narumi H, Kojima K, Nawa Y, Hara M. Hyponatremia during administration of tacrolimus in an allogeneic bone marrow transplant recipient. *Int J Hematol* 2003; **78**: 268–269.

Available online at www.sciencedirect.com
ScienceDirect
Blood Cells, Molecules, and Diseases 40 (2008) 410–413
BLOOD CELLS, MOLECULES, & DISEASES
www.elsevier.com/locate/ybcmd

The first confirmed case with C3 deficiency caused by compound heterozygous mutations in the *C3* gene; a new aspect of pathogenesis for C3 deficiency

Miyuki Kida [a], Hirotaka Fujioka [b], Yoshiyuki Kosaka [c], Kouhei Hayashi [c], Yukio Sakiyama [d], Tadashi Ariga [a,*]

[a] *Department of Pediatrics, Hokkaido University Graduate School of Medicine, N-15, W-7, Kita-ku, Sapporo, Hokkaido, Japan*
[b] *Department of Plastic Surgery, Bibai Rousai Hospital, Hokkaido, Japan*
[c] *Department of Hematology and Oncology, Hyogo Prefectural Kobe Children's Hospital, Hyogo, Japan*
[d] *Department of Human Gene Therapy, Hokkaido University Graduate School of Medicine, Hokkaido, Japan*

Submitted 29 October 2007
Available online 16 January 2008
(Communicated by R.I. Handin, M.D., 2 November 2007)

Abstract

The complement system is an ancient cascade system that has a major role in innate and adaptive immunity. Component C3 is central to the three complement pathways. Hereditary compliment 3 (C3) deficiency characterized by severe recurrent infections and immune complex disorders is extremely rare disease. Since 1972, inherited C3 deficiency has been described in many families representing a variety of national origins; however, only 8 families of these cases have been identified their genetic defects. Interestingly, all except one (incomplete analysis) were shown to harbor homozygous *C3* gene mutations. Previously we proposed a hypothesis, based on the unique process of C3 synthesis; C3 deficiency is not inherited as a simple autosomal recessive trait. Here, we report the first confirmed case with C3 deficiency caused by compound heterozygous mutations. They were a novel one base insertion (3176insT) in exon 24 which is predicted to result in a frameshift and a premature downstream stop codon (K1105X) in exon 26, and a nonsense mutation of C3303G (Y1081X) in exon 26 which was previously reported as homozygous mutations. This confirmed case suggests that our proposed hypothesis has prospects of a new aspect of pathogenesis for C3 deficiency.

Keywords: Component C3; C3 deficiency; Compound heterozygous mutations

Introduction

Complement protein C3 (OMIM+120700) is the major protein in the complement system in plasma. Cloning of the *C3* gene (19p13.3–13.2) revealed that the precursor molecule consists of 1663 amino acids encompassed by 41 exons and is located on chromosome 19. Inherited deficiency of C3 is an extremely rare disease; thus far, only 10 patients from eight families have had their molecular defects identified which led to their C3 deficiency [1–8]. It is notable that almost all mutations, which vary among each family group, were homozygous [1–4,6–8]. At present, only two cases (from one family) were suspected as being caused by compound heterozygous mutations after an incomplete analysis [5]. C3 is synthesized through a unique process; the mature C3 molecule results from a C3 precursor, which is cleaved into the α and β chains, and then the two chains are subsequently liked by disulfide bonds [9]. Previously, we reported the 10th case with C3 deficiency that was due to a novel homozygous mutation, and proposed a pathogenetic hypothesis, based on the unique process of C3 synthesis, that C3 deficiency is not inherited as a simple autosomal recessive trait [3]. Some compound heterozygous mutations, such as some combinations of missense mutations

* Corresponding author. Fax: +81 11 706 7898.
E-mail address: tada-ari@med.hokudai.ac.jp (T. Ariga).

1079-9796/$ - see front matter © 2007 Elsevier Inc. All rights reserved.
doi:10.1016/j.bcmd.2007.11.002

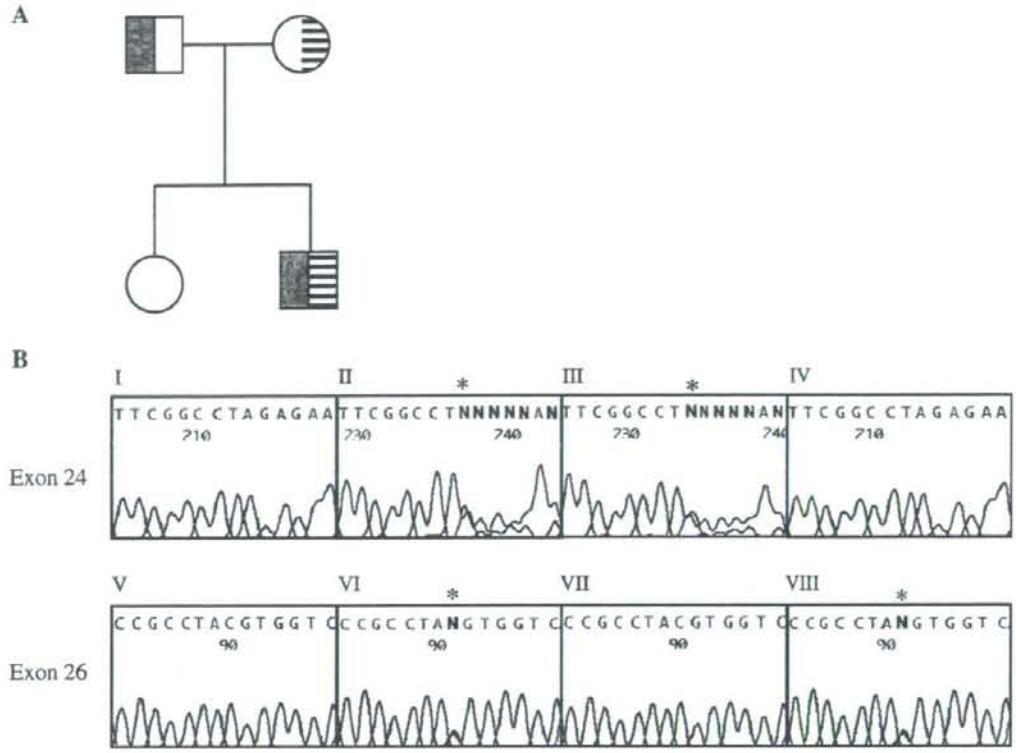

Fig. 1. (A) Pedigree of the family with C3 deficiency in this study. The patient was revealed to have compound heterozygous *C3* gene mutations with a paternal mutation (indicated as dark shadings) and a maternal mutation (indicated as horizontal strips). (B) Sequencing analysis of the patient with C3 deficiency and his family members I–IV: Sequence of a portion of exon 24 in the *C3* gene; normal individual (I), patient (II), patient's father (III) and patient's mother (IV). The mutation, derived from his father (indicated as dark shading in A) is a 1-bp insertion (3176insT) (asterisk mark indicates insertion point). V–VIII: Sequence of a portion of exon 26 in the *C3* gene; normal individual (V), patient (VI), patient's father (VII) and patient's mother (VIII). The mutation derived from his mother (indicated as horizontal strips in A) is a nonsense mutation described as C3303G (Y1081X) (asterisk mark indicates the mutated nucleotide).

affecting the different chains, can be compensated for by binding of the remaining wild type and the functionally normal α and β chains from the different alleles to avoid a more severe C3 deficiency. This hypothesis seemed consistent with the unexpected findings in hereditary C3 deficiency; its extremely rare occurrence and high ratio of homozygous mutation occurrence.

Case report

The pedigree of C3 deficiency is shown in Fig. 1A. The patient is a 2-year-old Japanese boy, who had suffered from several bacterial infections, such as meningitis, bronchitis and pneumonia. His parents and 5-year-old sister were all in good health. The parents were not related. Laboratory findings of the patient at this time were as follows: undetectable serum C3 level (<2 mg/dl; normal range, 75–150 mg/dl) and low CH50 (<12 U/ml; normal range, 35–45 U/ml). Blood examination of family members revealed that their serum C3 levels were 46 mg/dl in the father, 51 mg/dl in the mother and normal level in the sister, respectively. Serum CH50 levels were 33 U/ml in the father and 23 U/ml in the mother. Serum C4 levels in these family members were all within the normal range.

Materials and methods

Informed consent was obtained from his parents. Genomic DNA from family members, as well as from control individuals, was PCR-amplified for over the entire coding sequence of the *C3* gene including all its exon–intron boundaries using appropriate primers. PCR amplification products were purified using a QIAEX II Gel Extraction Kit (Qiagen) and directly sequenced in both directions using ABI PRISM 310 Genetic Analyzer (Applied Biosystems, Foster City, CA, USA).

Results and discussion

The patient was shown to have compound heterozygous *C3* gene mutations as shown in the Fig. 1B. They were a novel one base insertion (3176insT) in exon 24 which is predicted to result